Applied Physics A (2018) 124:522
https://doi.org/10.1007/s00339-018-1943-4

Applied Physics A
Materials Science & Processing

A facile and efficient strategy for the functionalization of multiple-walled carbon nanotubes using well-defined polypropylene-grafted polystyrene

Mojtaba Abbasian[1] · Haleh Ghaeminia[1] · Mehdi Jaymand[2]

Received: 25 April 2018 / Accepted: 26 June 2018 / Published online: 5 July 2018

Abstract
An alternative and efficient strategy for the synthesis of polymer-modified multiple-walled carbon nanotubes (MWCNTs) using ''grafting to'' technique was demonstrated successfully. For this purpose, maleic anhydride was grafted onto polypropylene (PP) followed by opening of anhydride ring with ethanolamine to produce hydroxylated polypropylene (PP-OH). The hydroxyl groups were esterified using α-phenyl chloroacetyl chloride to obtain PP-Cl macroinitiator. Afterward, styrene (St) monomer was grafted onto PP through atom transfer radical polymerization technique to afford PP-*g*-PSt graft copolymer. The chloride-end-caped PP-*g*-PSt copolymer was then attached to the oxidized MWCNTs in the presence of CuBr as the catalyst to produce MWCNTs-*g*-(PP-*g*-PSt) nanocomposite. The chemical structures of all samples as representatives were characterized by means of Fourier transform infrared spectroscopy. The chemical attaching of PP-*g*-PSt to the MWCNTs was approved by thermal property study using thermogravimetric analysis and differential scanning calorimetry, as well as morphology studies using transmission electron and scanning electron microscopies. The synthesized MWCNTs-*g*-(PP-*g*-PSt) nanocomposite can be applied as a reinforcement for polymeric (nano-)composites due to superior features of MWCNTs as well as their compatibility with polymeric materials after functionalization processes.

1 Introduction

Since the discovery of carbon nanotubes (CNTs) by Iijima [1], more and more attention have been devoted for application of this nanomaterial in various industrial and biological fields. This nanomaterial possesses some superior physicochemical features including nanometer size, good chemical stability, high aspect ratios, excellent mechanical strength, as well as high thermal and electrical conductivity [2–4]. The most important application fields of CNTs can be listed as bio/chemical sensors [5], energy storage [6], field emission materials [7], electronic devices [8], catalyst support [9], as a reinforcement for polymeric materials [2, 4], as well as biomedical fields [10].

In general, the homogeneous dispersion of CNTs in polymeric matrix is hindered by both synthesis-induced 'entangled' and 'aggregated' structures of nanotubes, as well as the tube tendency to form agglomerates, mainly due to the strong intermolecular van der Waals interactions between individual CNTs [11–13]. In the case of polymeric nanocomposites based on CNTs, it is well established that the physicochemical and mechanical features of resultant material are strongly depend on the dispersion of CNTs in polymer matrix [14]. Therefore, improvement in their compatibility with monomers and polymers is necessary toward fabrication of nanocomposites with proper physicochemical properties. In this context, CNTs can be modified using both chemical [15, 16], and physical [17, 18] approaches. Carboxylation of CNTs is the most commonly used chemical approach to produce stable water dispersion of nanotubes and for further modification through carboxylic groups [19, 20]. Among the various approaches for the modification of oxidized CNTs, the polymer grafting is particular of interest. In this context, the main methods for macromolecules attaching are ''grafting from'' and ''grafting to'' techniques. The ''grafting from'' mechanism promises high graft densities; however, immobilization of initiators onto CNTs and

✉ Mehdi Jaymand
m_jaymand@yahoo.com; m.jaymand@gmail.com; jaymandm@tbzmed.ac.ir

[1] Department of Chemistry, Payame Noor University, P.O. Box 19395-3697, Tehran, Iran

[2] Immunology Research Center, Tabriz University of Medical Sciences, Tabriz, Iran

control over molecular weight and architecture can be difficult to achieve. In the case of ''grafting to'' technique, a polymer with a specific molecular weight and well-known architecture can be synthesized and attached to the graphitic surface of CNTs through end-group transformation [14, 19, 20].

In recent years, many researchers have attempted to utilize reversible deactivation radical polymerization (RDRP) technique for the synthesis of CNTs-based nanocomposites with well-defined structures [21–23]. This approach is divided into three main categories including atom transfer radical polymerization (ATRP) [24, 25], nitroxide-mediated radical polymerization (NMRP) [26, 27], and reversible addition of fragmentation chain transfer (RAFT) polymerization [28, 29]. Among these, ATRP is a robust and efficient approach to accurately control the molecular weight, architecture and, dispersity of the synthesized polymer. Other advantages of ATRP technique are negligible homopolymer formation when employed in graft copolymerization, as well as its applicability to numerous monomers possessing various functional groups and polarities. In addition, this technique is simple and has excellent tolerance to many solvents, additives, and impurities [30, 31].

The objective of this research was to design and develop an efficient and simple approach for the synthesis of well-defined polymer-grafted multiple-walled carbon nanotubes (MWCNTs) using ''grafting to'' technique. For this purpose, polypropylene (PP) was functionalized using α-phenyl chloroacetyl chloride to obtain PP-Cl macroinitiator. Then, styrene (St) monomer was grafted onto PP through ATRP technique to afford a PP-*g*-PSt graft copolymer. The chloride-end-caped PP-*g*-PSt copolymer was then attached to the oxidized MWCNTs in the presence of CuBr as the catalyst to afford MWCNTs-*g*-(PP-*g*-PSt) nanocomposite.

2 Experimental

2.1 Materials

MWCNTs (purity ˃ 95%) with an average diameter and length of about 10–20 nm and 20 μm, respectively, were purchased from Research Institute of Petroleum Industry (Tehran, Iran), and purified as described in 2.6. section. Copper(I) chloride (Merck, Darmstadt, Germany) was purified by stirring in glacial acetic acid, then washed with methanol, and finally dried under reduced pressure at room temperature. Styrene monomer (Tabriz Petrochemical Co., Tabriz, Iran) dried over calcium hydride (CaH_2), distilled under reduced pressure, and then stored at − 20 °C prior to use. *O*-Xylene and toluene (Merck) were dried by refluxing over sodium and distilled under argon prior to use. Isotactic polypropylene (i-PP; P SF060) was obtained from Polynar Company (Tabriz, Iran), and was used as received. Maleic anhydride (MA), 2, 2′-bipyridine (BPy), trimethylamine, α-phenyl chloroacetyl chloride, and ethanolamine were purchased from Sigma-Aldrich (St. Louis, MO, USA) and were used as received. All other reagents and solvents were purchased from Merck or Sigma-Aldrich and purified according to the standard methods.

2.2 Synthesis of PP-*g*-MA

The reaction of MA with PP was carried out as follows. A 100-mL three-neck round-bottom flask equipped with condenser, gas inlet/outlet, and a magnetic stirrer was charged with PP (5.00 g), MA (2.00, 20 mmol), and dried *O*-xylene (80 mL). The reaction mixture was de-aerated by bubbling highly pure argon for some minutes, and then allowed the temperature which was increased to 60 °C for about 2 h to make the PP particles swell. In a separate container, benzoyl peroxide (0.10 g, 0.40 mmol) was dissolved in dried xylene (10 mL), de-aerated by bubbling highly pure argon for some minutes, and then dropped into the reaction flask during 15 min. The content of the flask was warmed to 120 °C and stirred for about 3 h. At the end of this time, the product was poured into warm water (500 mL), filtered, and washed with a large amount of warm water until pH 7. Finally, the obtained PP-*g*-MA (6.15 g) was washed with acetone and dried at 50 °C for 24 h in vacuum.

2.3 Synthesis of PP-OH

The synthesized PP-*g*-MA was reacted with ethanolamine in a 100-mL glass reactor equipped with condenser, gas inlet/outlet, and a magnetic stirrer. The reactor was charged with PP-*g*-MA (5.00 g) and *O*-xylene (70 mL). The reaction mixture was de-aerated by bubbling highly pure argon for some minutes, and then stirred at 120 °C for about 2 h. Afterward, ethanolamine (2.50 mL, 41 mmol) was added to the reactor using a syringe through the septum, and the reaction mixture was maintained at 120 °C for 6 h under argon protection. The reaction was terminated through the pouring of reaction mixture into 300 mL of acetone. The precipitated polymer was collected by filtration, washed with acetone, and dried in reduced pressure at 60 °C to give hydroxylated PP (PP-OH) as a white powder (Scheme 1) [32].

2.4 Synthesis of PP-Cl macroinitiator

A 100-mL glass reactor equipped with condenser, gas inlet/outlet, septum, and a magnetic stirrer. The reactor was charged with PP-OH (4.00 g) and dried toluene (60 mL). The content of the reactor was warmed up to 100 °C using an oil bath under stirring (2 h) to swell and dispersion of PP-OH. The content of the flask was cooled, added triethylamine

Scheme 1 Overall strategy for the synthesis of PP-*g*-MA and PP-OH

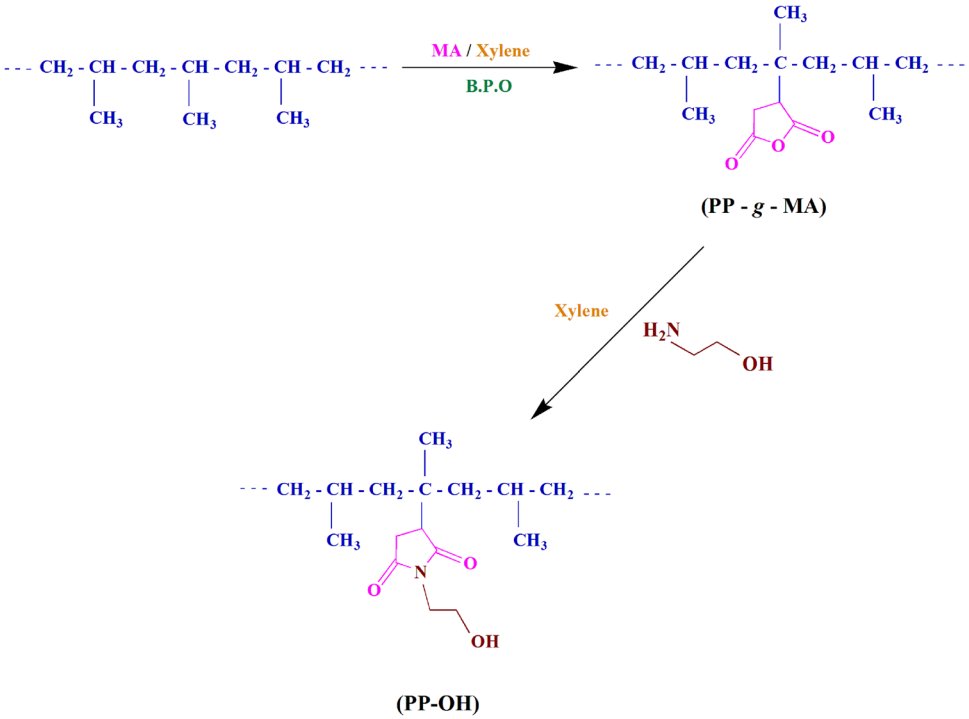

(1.50 mL, 17 mmol), and the reaction mixture was de-aerated by bubbling highly pure argon for some minutes. Afterward, α-phenyl chloroacetyl chloride (2.70 mL, 17 mmol) was added to the reaction mixture using a syringe through the septum, and the content of the reactor was stirred for about 2 h at room temperature. Then, the flask was warmed to 100 °C using an oil bath, and the reaction mixture was stirred for another 5 h under argon protection. At the end of this time, the reaction mixture was cooled using an ice/water bath, and poured into a large amount of cold methanol. The resulting polymer was collected by filtration, washed with methanol several times, and dried in vacuum at room temperature [32].

2.5 Graft copolymerization of styrene onto PP-Cl macroinitiator using ATRP technique

A polymerization ampoule was charged with PP-Cl (3.00 g), CuCl (0.10 g, 0.10 mmol), BPy (0.25 g, 0.15 mmol), styrene monomer (4.6 mL, 40 mmol), and dried *O*-xylene (15 mL). The ampoule was degassed with several freeze–pump–thaw cycles, sealed off under vacuum, and placed in an oil bath at 100 °C for about 15 h. At the end of this period, the ampoule was cooled using an ice–water bath, to stop the polymerization. The content of the ampoule was precipitated into cold methanol (200 mL) and filtered, and the product was dried in vacuum at 50 °C [33]. The crude product was extracted with xylene at room temperature three times, to remove PSt homopolymer. The purified product was dried in a vacuum at 50 °C and weighed (5.85 g) (Scheme 2).

2.6 Stepwise purification of MWCNTs

The received pristine MWCNTs was purified thermally and chemically to remove foreign impurities. The amorphous carbon was removed through thermal oxidation of MWCNTs at 550 °C in air flowing for 30 min. The chemical purification was consecutively done with HCl (6 M) and HNO_3 (6 M) solutions, respectively, under stirring for about 3 h [20].

2.7 Synthesis of MWCNTs–COOH

A 100-mL round-bottom glass reactor equipped with condenser, and a magnetic stirrer was charged with purified MWCNTs (0.50 g), and a mixture (1:3 v/v) of sulfuric acid (15 mL, 95–97%) and nitric acid (45 mL, 65%). The content of the reactor was sonicated for about 1 h to open agglomeration of nanotubes and anchoring acid solution uniformly on the CNTs surface. Afterward, the homogenized MWCNTs dispersion was oxidized under reflux at 100 °C for about 7 h to introduce functional carboxyl acid groups. At the end of this time, fivefold dilution was then applied to the mixture to stop oxidation reaction. The product was washed using distilled water until the water pH approximately at 7. The product was dried in vacuum at 50 °C, and assigned as carboxylated MWCNTs (MWCNTs–COOH) [20].

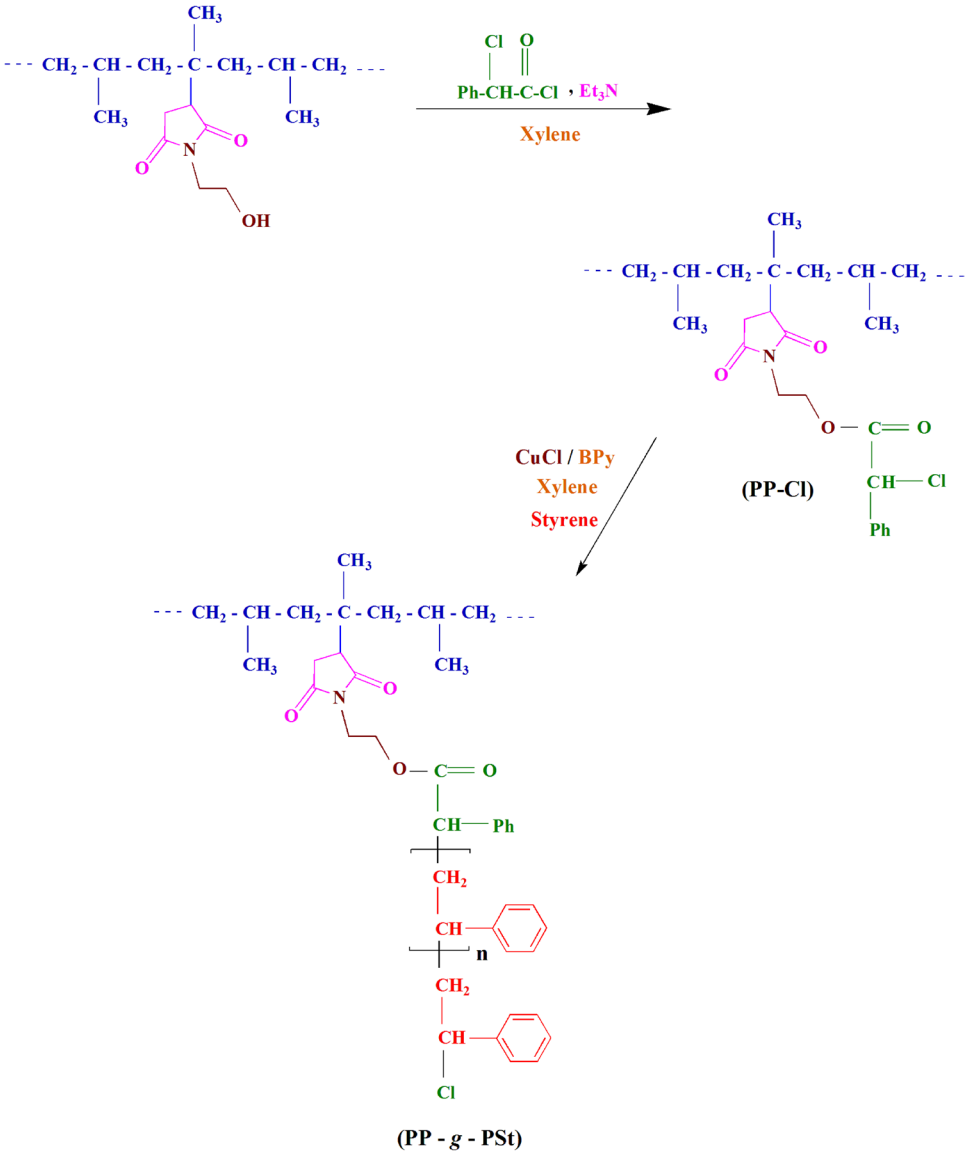

Scheme 2 Overall strategy for the synthesis of PP-Cl macroinitiator and PP-*g*-PSt copolymer

2.8 Synthesis of MWCNTs-*g*-(PP-*g*-PSt)

MWCNTs–COOH (100 mg) was dispersed in xylene (20 mL) through the sonication for about 20 min. Then, the PP-*g*-PSt copolymer (1.00 g) and CuBr(I) (7 mg, 0.05 mmol) were added to the solution and sonicated again for another 15 min. The reaction mixture was transferred into a 50-mL round-bottom glass reactor and refluxed at 90 °C for about 12 h under argon protection. The resulting product was filtered, and extracted using hot toluene and xylene several times to remove un-grafted polymeric chains. The product obtained was then dried in vacuum at 60 °C (Scheme 3).

2.9 Characterization and analyses

Fourier transform infrared (FTIR) spectra of the samples were obtained on a Shimadzu 8101M FTIR (Shimadzu, Kyoto, Japan). The samples were prepared by grinding the dry powders with KBr and compressing the mixture into disks. Transmission electron microscopy (TEM) was performed using a Philips EM 208 microscope (Phillips, Eindhoven, The Netherlands) with a 100-kV accelerating voltage. The scanning electron microscope (SEM) type 1430 VP (LEO Electron Microscopy Ltd., Cambridge, UK) was applied to determine the morphologies of the synthesized samples at operating voltage of 15.00 kV. The thermal properties of the samples were obtained with a TGA-PL STA 1640 (Polymer Laboratories, Shropshire, UK). About 10 mg of the sample was heated between 25 and 600 °C at a rate of 10 °C/min under flowing nitrogen. Differential scanning calorimetry analyses were performed with a Netzsch (Selb, Germany)-DSC 200 F_3 Maia. The sample was first heated to 200 °C and then allowed to cool for 5 min to eliminate the thermal history. Thereafter, the sample was reheated to

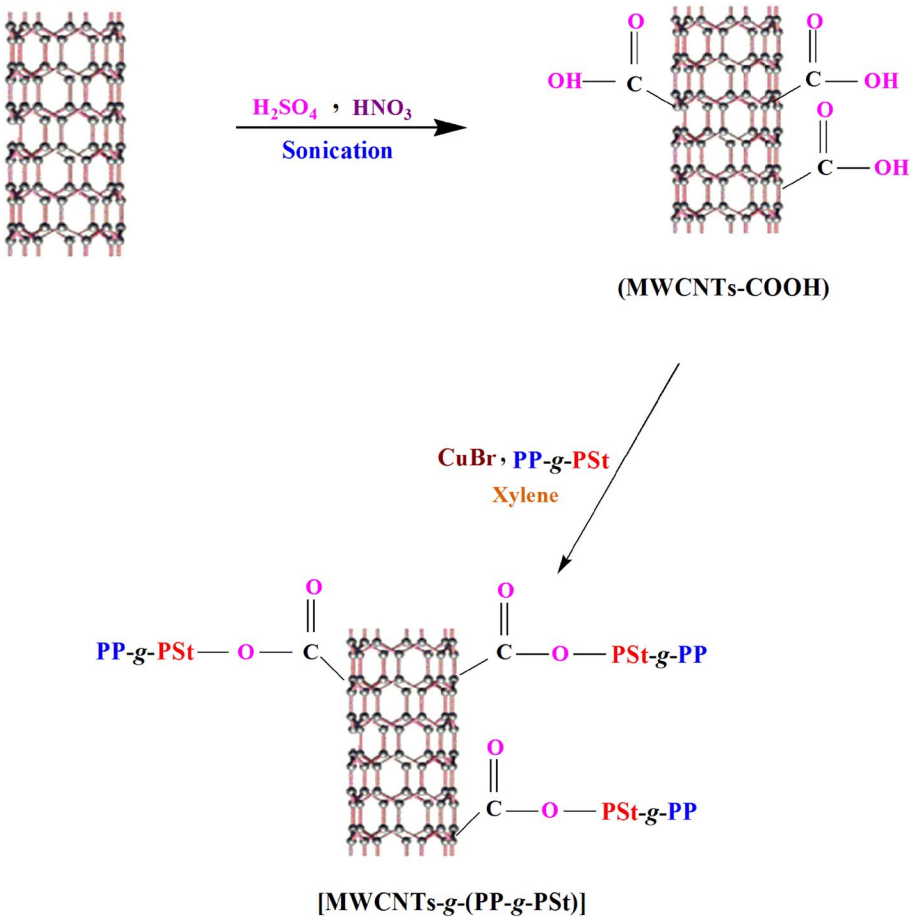

Scheme 3 Overall strategy for the synthesis of MWCNTs–COOH and MWCNTs-*g*-(PP-*g*-PSt) nanocomposite

200 °C at a rate of 10 °C/min. The entire test was performed under nitrogen purging.

3 Result and discussion

3.1 FTIR spectroscopy

All synthesized samples were characterized using FTIR spectroscopy, as shown in Figs. 1 and 2. The FTIR spectrum of the neat PP shows characteristic absorption bands of aliphatic C–H stretching vibrations at 2950–2800 cm^{-1} region, and bending vibrations of C–H at 1467 and 1376 cm^{-1}. The most important change after grafting of MA monomer onto PP is the appearance of new absorption bands at 1712 and 1783 cm^{-1} that corresponds to the symmetrical and asymmetrical stretching modes of anhydride groups in the MA unite. As seen in FTIR spectrum of PP-OH, the absorption bands of anhydride were shifted to 1714 and 1658 cm^{-1} due to reaction with ethanolamine and conversion to succinimide group. Additional important change in this spectrum is the appearance of hydroxyl stretching vibration as a broad band centered at 3470 cm^{-1} that corresponds to the ethanolamine moiety. The successful synthesis of PP-Cl macroinitiator is confirmed through the appearance of new absorption bands related to carbonyl group of α-phenyl chloroacetate moiety at 1783 cm^{-1}, as well as γ(C–H) in the aromatic ring of α-phenyl chloroacetate moiety at 836 and 758 cm^{-1}. In addition, as seen, the stretching vibration of hydroxyl group at 3470 cm^{-1} is disappeared completely that verifies the successful conversion of hydroxyl groups into α-phenyl chloroacetate moiety.

The FTIR spectrum of the pristine MWCNTs exhibited the weak asymmetric and symmetric stretching vibrations of the –CH groups at 2950–2800 cm^{-1} region, stretching vibration of carboxyl groups at 1736 cm^{-1}, and hydroxyl stretching vibration as a broad and strong band centered at 3480 cm^{-1}. It should be pointed out that the most portion of carboxyl groups in the pristine MWCNTs was formed during the chemical purification of CNTs. In the FTIR spectrum of the oxidized MWCNTs, the strong absorption band centered at 3480 cm^{-1} is related to the stretching vibration of –OH of carboxyl or hydroxyl groups. The stretching vibrations of C=O and C–O groups were appeared at 1728 and 1236 cm^{-1}, respectively.

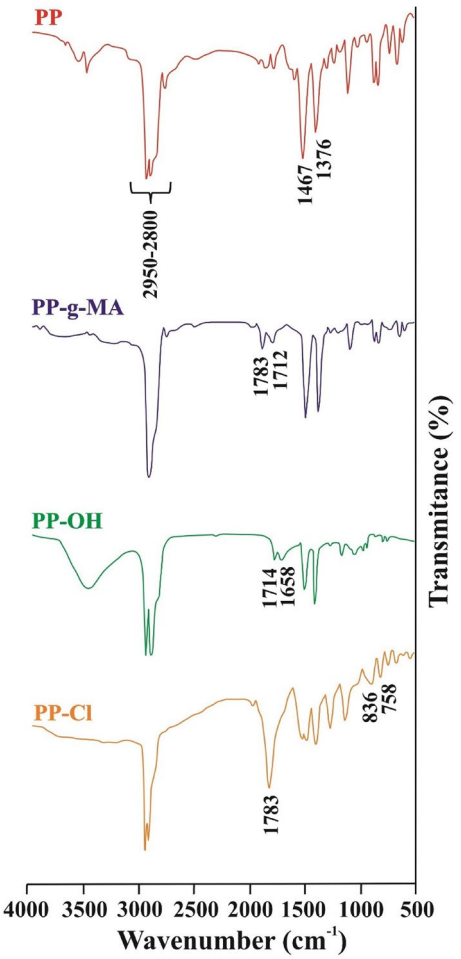

Fig. 1 FTIR spectra of neat PP, PP-*g*-MA, PP-OH, and PP-Cl

In comparison with the FTIR spectrum of the MWCNTs–COOH, the FTIR spectrum of the MWCNTs-*g*-(PP-*g*-PSt) exhibited some differences including the appearance of the stretching vibrations of aromatic and aliphatic –CH groups (related to PP-*g*-PSt) at 3050–2800 cm^{-1} region, as well as γ(C–H) in the aromatic ring (related to pendent phenyl rings of PSt) at 900–700 cm^{-1} region (Fig. 2).

3.2 Grafting parameters

The grafting parameters such as grafting efficiency, grafting yield, and weight gain for the synthesized PP-*g*-MA and PP-*g*-PSt copolymers were determined gravimetrically according to the following equations:

a. Grafting yield (%G) = $(W_g - W_0)/W_g \times 100$,
b. Grafting efficiency (%GE) = $W_g/(W_m + W_0) \times 100$,
c. Weight gain (%WG) = $(W_g - W_0)/(W_m + W_0) \times 100$.

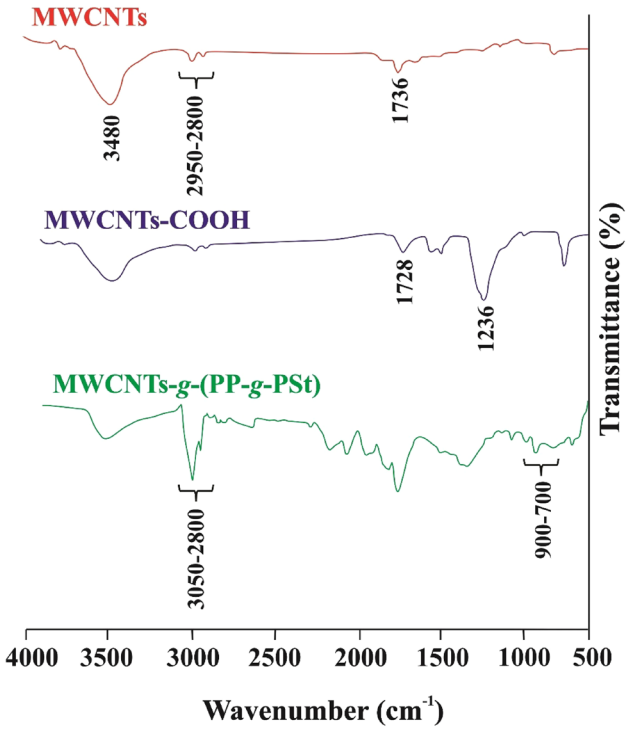

Fig. 2 FTIR spectra of pristine MWCNTs, MWCNTs–COOH, and MWCNTs-*g*-(PP-*g*-PSt)

In these equations W_g is the mass of PP-*g*-MA or PP-*g*-PSt copolymer, W_0 is the mass of initial PP or PP-Cl macroinitiator, and W_m is the mass of MA or styrene monomers taken for the reaction [34, 35]. The grafting parameters were calculated and summarized in Table 1.

3.3 Thermal property study

DSC is a powerful tool for the investigation of thermal properties of polymeric materials and determines transition temperatures such as glass transitions, melting, and decomposition. The DSC thermograms of neat PP, PP-*g*-MA, PP-*g*-PSt, and MWCNTs-*g*-(PP-*g*-PSt) are shown in Figs. 3 and 4. The DSC curve of the neat PP exhibited an endothermic peak at 159 °C related to the melting temperature (T_m) of this thermoplastic. In contrast, in the DSC curve of the PP-*g*-MA, the T_m value decreased slightly (151 °C) in comparison with neat PP due to grafting process. It may be resulted from

Table 1 Grafting parameters for the synthesized PP-*g*-MA and PP-*g*-PSt

Sample	Mass of grafting (W_g)	Weight gain (%WG)	Grafting efficiency (%GE)	Grafting yield (%G)
PP-*g*-MA	6.15	16.4	87.8	18.7
PP-*g*-PSt	5.85	39.7	81.5	48.7

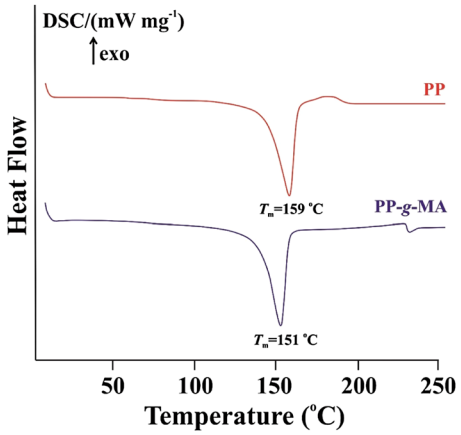

Fig. 3 DSC thermogram of PP and PP-*g*-MA

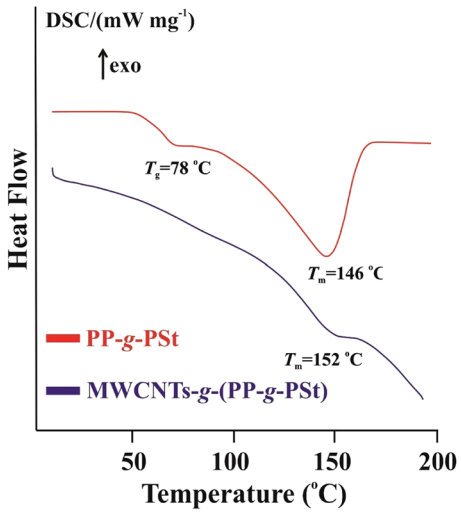

Fig. 4 DSC thermograms of PP-*g*-PSt copolymer and MWCNTs-*g*-(PP-*g*-PSt) nanocomposite

the grafted branches, which disrupted the regularity of the chain structures in PP and increased the spacing between the chains.

The DSC thermogram of PP-*g*-PSt copolymer exhibited a strong endothermic peak at 146 °C corresponding to the T_m of this copolymer that confirms the presence of PP in the copolymer. In addition, the T_g of the copolymer is observed at 78 °C. This T_g is related to the movement of polystyrene chains, and demonstrates the presence of microphage separation in this graft copolymer mainly due to immiscibility of PSt and PP. The T_m in the MWCNTs-*g*-(PP-*g*-PSt) nanocomposite is increased to 152 °C mainly due to presence of MWCNTs. It should be pointed out that the T_g is not detected in this sample.

The characteristic TGA curves of pristine MWCNTs, neat PP, and MWCNTs-*g*-(PP-*g*-PSt) nanocomposite is shown in Fig. 5. As seen, the pristine MWCNTs are stable till 450 °C, and after this temperature, CNTs exhibited a negligible weight loss up to 600 °C. The residue at 600 °C for pristine MWCNTs is about 97 wt%. The pure PP is started to decomposition in one step at around 350–440 °C, and after which the loss rate slows down. The residue at 600 °C for pure PP is about 3 wt%.

The TGA thermogram of MWCNTs-*g*-(PP-*g*-PSt) nanocomposite exhibits a two-step weight loss process; the initial weight loss at 280–310 is related to the decomposition of small molecules, whereas the second step at around 330–510 °C. The weight loss at lower temperatures (330–380 °C) is related to the decomposition of PSt chains, and weight loss at higher temperatures (380–510 °C) is related to decomposition of PP chains, after which the loss rate slows down. The residue at 600 °C for nanocomposite is about 11 wt%. In addition, the presence of MWCNTs increased the thermal stability of the PP-*g*-PSt copolymer [36].

3.4 Morphology study

Direct and clear evidence regarding the attaching of PP-*g*-PSt copolymer to the MWCNTs was obtained not only using TGA and FTIR spectroscopy but also from SEM and TEM observations. The SEM images of pristine MWCNTs and MWCNTs-*g*-(PP-*g*-PSt) nanocomposite are shown in Fig. 6. As seen, the pristine MWCNTs consisting of agglomerated carbon nanotubes (Fig. 6a). In contrast, the SEM image of MWCNTs-*g*-(PP-*g*-PSt) nanocomposite exhibited that the surface of CNTs was covered by polymeric chains. However, some agglomeration of MWCNTs still exists, although the generally excellent separation of MWCNTs is attributed to the attaching of PP-*g*-PSt chains, which separates the previously agglomerated MWCNTs (Fig. 6b).

More evidence on the attaching of PP-*g*-PSt copolymer to the MWCNTs was obtained using TEM observation. TEM images of pristine MWCNTs, MWCNTs–COOH, and

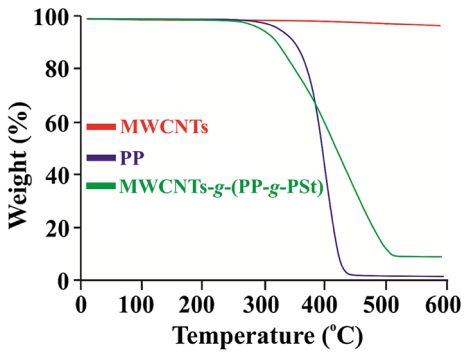

Fig. 5 TGA curves of MWCNTs, PP-*g*-PSt copolymer, and MWCNTs-*g*-(PP-*g*-PSt) nanocomposite

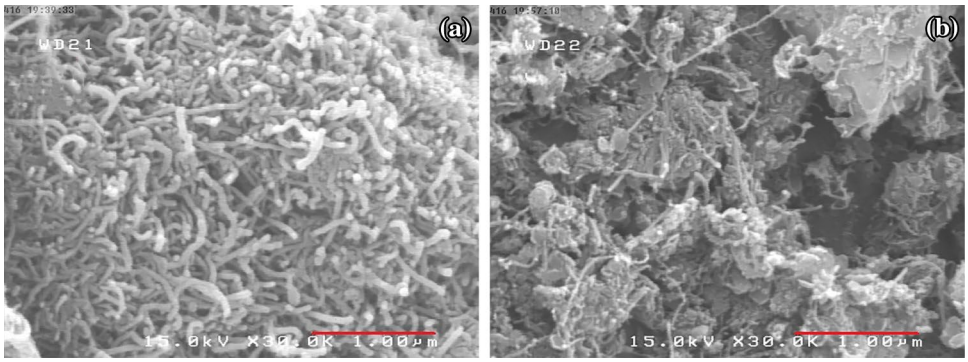

Fig. 6 SEM images of pristine MWCNTs (**a**) and MWCNTs-*g*-(PP-*g*-PSt) nanocomposite (**b**)

MWCNTs-*g*-(PP-*g*-PSt) nanocomposite are shown in Fig. 7. In accordance with SEM image, the TEM image of pristine MWCNTs exhibited agglomerated CNTs mainly due to high aspect ratio and strong interaction between individual nanotubes (Fig. 7a). The TEM image of MWCNTs–COOH exhibited that the agglomeration is decreased significantly after oxidizing of MWCNTs. However, some agglomeration of MWCNTs still exists in the case of this sample (Fig. 7b).

The TEM images of MWCNTs-*g*-(PP-*g*-PSt) nanocomposite revealed that some parts of the tubes were covered with the PP-*g*-PSt copolymer layer (Fig. 7c, d). Both TEM images give thickness diameter distribution in the range of 10–20 nm. In addition, the grafting of the copolymer takes place along the MWCNTs, not just on their tips. As seen, the graphitic-like structure of the MWCNTs is preserved after all the functionalization processes [37].

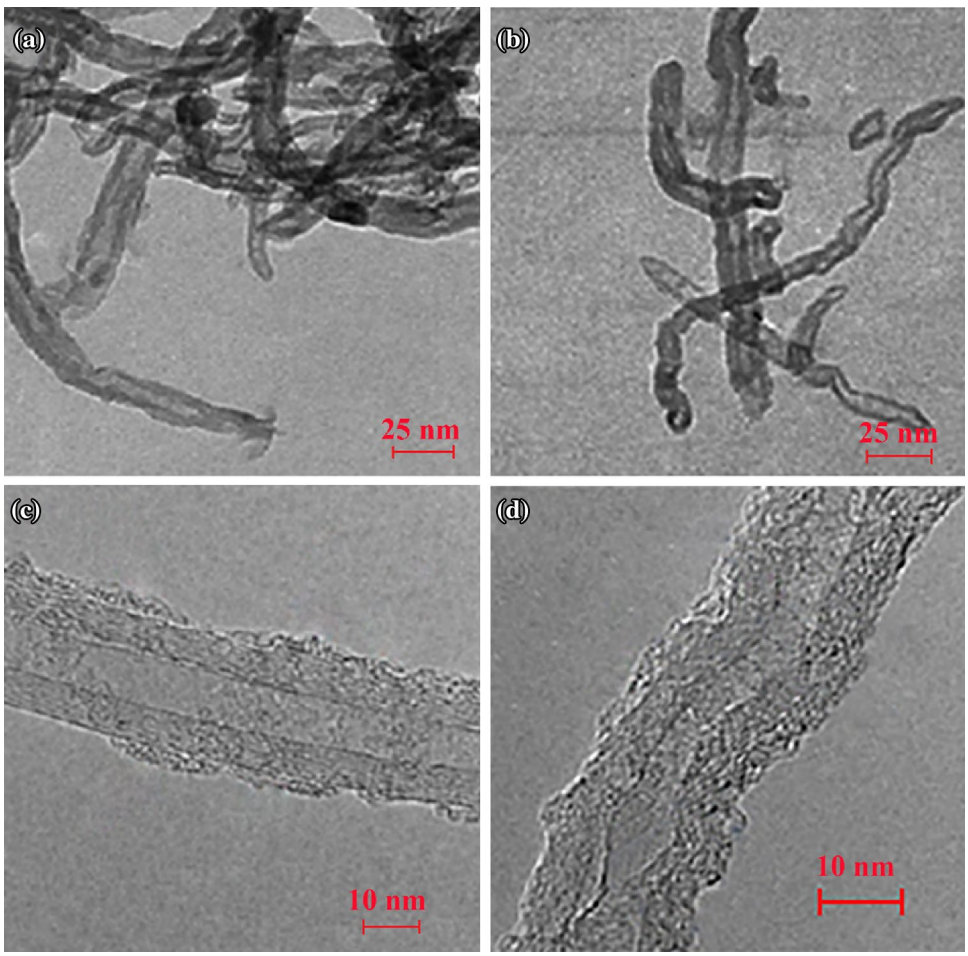

Fig. 7 TEM images of pristine MWCNTs (**a**), MWCNTs–COOH (**b**), and MWCNTs-*g*-(PP-*g*-PSt) nanocomposite (**c, d**)

4 Conclusions

An efficient approach for the chemical modification of MWCNTs was demonstrated successfully through the combination of ATRP and ''grafting to'' techniques. For this purpose, PP was grafted with styrene monomer using ATRP technique, and the resultant halide end-capped well-defined graft copolymer was grafted to the MWCNTs through the metal catalyzed atom transfer approach. The chemical structures of all synthesized samples as representatives were confirmed using FTIR spectroscopy. Thermal property study using TGA and DSC as well as SEM and TEM observations provided direct and clear evidence for grafting of PP-*g*-PSt to the MWCNTs.

We believe that the employed strategy can be applied in the synthesis of other polymer coated CNTs with increasing complexity and functionality in the polymeric shells, due to its simplicity, and applicability for wide variety of monomers with various functionalities. In addition, the synthesized MWCNTs-*g*-(PP-*g*-PSt) has potential as a reinforcement for polymeric (nano-)composites due to excellent physicochemical and mechanical properties of MWCNTs as well as their compatibility with polymeric materials after functionalization processes.

Acknowledgements The authors express their sincere thanks to Payame Noor University, Tehran, Iran, and Tabriz University of Medical Sciences, Tabriz, Iran for the financial support of this work.

Compliance with ethical standards

Conflict of interest The authors declare that they have no competing interests.

References

1. S. Iijima, Nature **354**, 56 (1991)
2. C. Oueiny, S. Berlioz, F.X. Perrin, Prog. Polym. Sci. **39**, 707 (2014)
3. J.L. Blackburn, A.J. Ferguson, C. Cho, J.C. Grunlan, Adv. Mater. **30**, 1704386 (2018)
4. M.S. Balogun, Y. Luo, W. Qiu, P. Liu, Y. Tong, Carbon **98**, 162 (2016)
5. J. Budhathoki-Uprety, R.E. Langenbacher, P.V. Jena, D. Roxbury, D.A. Heller, ACS Nano **11**, 3875 (2017)
6. A.A. Arrocha-Arcos, M. Miranda-Hernández, Int. J. Hydrog. Energy. **43**, 7372 (2018)
7. S. Huang, W. Li, L. Zhu, M. He, Z. Yao, Y. Zhou, X. Xu, Z. Ren, J. Bai, Carbon **132**, 335 (2018)
8. G. Zhang, S. Jiang, W. Yao, C. Liu, ACS Appl. Mater. Interfaces **8**, 31202 (2016)
9. J.C. Li, P.X. Hou, C. Liu, Small **13**, 1702002 (2017)
10. V. Biju, Chem. Soc. Rev. **43**, 744 (2014)
11. A. Hirsch, Angew. Chem. Int. Ed. **41**, 1853 (2002)
12. Y.J. Lee, S.R. Ham, J.H. Kim, T.H. Yoo, S.R. Kim, Y.T. Lee, D.K. Hwang, B. Angadi, W.S. Seo, B.K. Ju, W.K. Choi, Sci. Rep. **8**, 4851 (2018)
13. P.S. Omurtag, B. Alkan, H. Durmaz, G. Hizal, U. Tunca, Polymer **141**, 213 (2018)
14. J. Abraham, J. Thomas, N. Kalarikkal, S.C. George, S. Thomas, J. Phys. Chem. B **122**, 1525 (2018)
15. A. Bensghaïer, S.L. Truong, M. Seydou, A. Lamouri, E. Leroy, M. Mičušik, K. Forro, M. Beji, J. Pinson, M. Omastová, M.M. Chehimi, Langmuir **33**, 6677 (2017)
16. F. Ren, H. Yu, L. Wang, RSC Adv. **4**, 14419 (2014)
17. M.S. Ata, R. Poon, A.M. Syed, J. Milne, I. Zhitomirsky, Carbon **130**, 584 (2018)
18. R.C. Selhorst, E. Puodziukynaite, J.A. Dewey, P. Wang, M.D. Barnes, A. Ramasubramaniam, T. Emrick, Chem. Sci. **7**, 4698 (2016)
19. B. Massoumi, M. Ramezami., M. Jaymand, M. Ahmadinejad, J. Polym. Res. **22**, 214 (2015)
20. B. Massoumi, M. Jaymand, R. Samadi, A.A. Entezami, J. Polym. Res. **21**, 442 (2014)
21. H. Kong, W. Li, C. Gao, D. Yan, Y. Jin, D.R.M. Walton, Macromolecules **37**, 6683 (2004)
22. D.Q. Fan, J.P. He, W. Tang, J.T. Xu, Y.L. Yang, Eur. Polym. J. **43**, 26 (2007)
23. J. Gupta, D.J. Keddie, C. Wan, D.M. Haddleton, T. McNally, Polym. Chem. **7**, 3884 (2016)
24. R. Mohammad-Rezaei, B. Massoumi, M. Abbasian, M. Jaymand, J. Polym. Res. **25**, 93 (2018)
25. B. Massoumi, F. Ghandomi, M. Abbasian, M. Eskandani, M. Jaymand, Appl. Phys. A **122**, 1000 (2016)
26. S.G. Karaj-Abad, M. Abbasian, M. Jaymand, Carbohyd. Polym. **152**, 297 (2016)
27. J. Nicolasa, Y. Guillaneuf, C. Lefay, D. Bertin, D. Gigmes, B. Charleux, Prog. Polym. Sci. **38**, 63 (2013)
28. F. Mahmoodzadeh, M. Abbasian, M. Jaymand, A. Amirshaghaghi, Polym. Int. **66**, 1651 (2017)
29. J.T. Sun, C.Y. Hong, C.Y. Pan, Polym. Chem. **4**, 873 (2013)
30. B. Massoumi, Z. Mozaffari, M. Jaymand, Int. J. Biol. Macromol. **117**, 418 (2018)
31. M. Abbasian, M. Pakzad, K. Nazari, Polym. Plast. Technol. Eng. **56**, 857 (2017)
32. M. Abbasian, M. Shahparian, S.E.S. Bonab, Iran. Polym. J. **22**, 209 (2013)
33. M. Hatamzadeh, M. Jaymand, RSC Adv. **4**, 16792 (2014)
34. M. Jaymand, Polym. Plast. Technol. Eng. **51**, 514 (2012)
35. M. Jaymand, Macromol. Res. **19**, 998 (2011)
36. M. Abbasian, S.Y. Fathi, J. Polym. Eng. **33**, 463 (2013)
37. S. Bhattacharyya, C. Sinturel, O. Bahloul, M.L. Saboungi, S. Thomas, J.P. Salvetat, Carbon **46**, 1037 (2008)